D.A.Φ.N.E.*
DESIGN CRITERIA AND PROJECT OVERVIEW

The DAΦNE Project Team**
presented by G. Vignola
INFN, Laboratori Nazionali di Frascati, C.P. 13, 00044 Frascati (Rome), Italy

ABSTRACT

The basic design criteria of DAΦNE, the Frascati Φ-factory, are discussed and a project overview is presented.

INTRODUCTION

The DAΦNE project of the INFN Frascati National Laboratories consists in the construction of a two rings colliding beam Φ-Factory and a 510 MeV e^+/e^- injector for topping-up. The initial luminosity goal is:

$$L = 10^{32}\ cm^{-2}\ sec^{-1}$$

while the final luminosity target is:

$$L \sim 10^{33}\ cm^{-2}\ sec^{-1}.$$

The project has been approved and funded by the INFN Board of Directors in June 1990. The engineering design has started in January 1991; construction and commissioning is scheduled for the end of 1995. A general layout of the complex, inside the existing LNF buildings, is shown in Fig. 1.

DESIGN PHILOSOPHY

It is important, in the context of this workshop, to discuss:

- How DAΦNE will reach luminosities in the $10^{32} \div 10^{33}$ range.
- If the luminosity goals are realistic.

---

* Double Annular Φ-factory for Nice Experiments.

** P. Amadei, A. Aragona, S. Bartalucci, M. Bassetti, M.E. Biagini, C. Biscari, R. Boni, A. Cattoni, V. Chimenti, A. Clozza, S. De Simone, G. Di Pirro, S. Faini, R. Fedele, A. Gallo, A. Ghigo, S. Guiducci, H. Hsieh, S. Kulinski, M.R. Masullo, C. Milardi, M. Modena, L. Palumbo, M. Preger, G. Raffone, C. Sanelli, M. Serio, F. Sgamma, B. Spataro, A. Stecchi, L. Trasatti, C. Vaccarezza, V.G. Vaccaro, M. Vescovi, S. Vescovi, G. Vignola, J. Wang, M. Zobov.

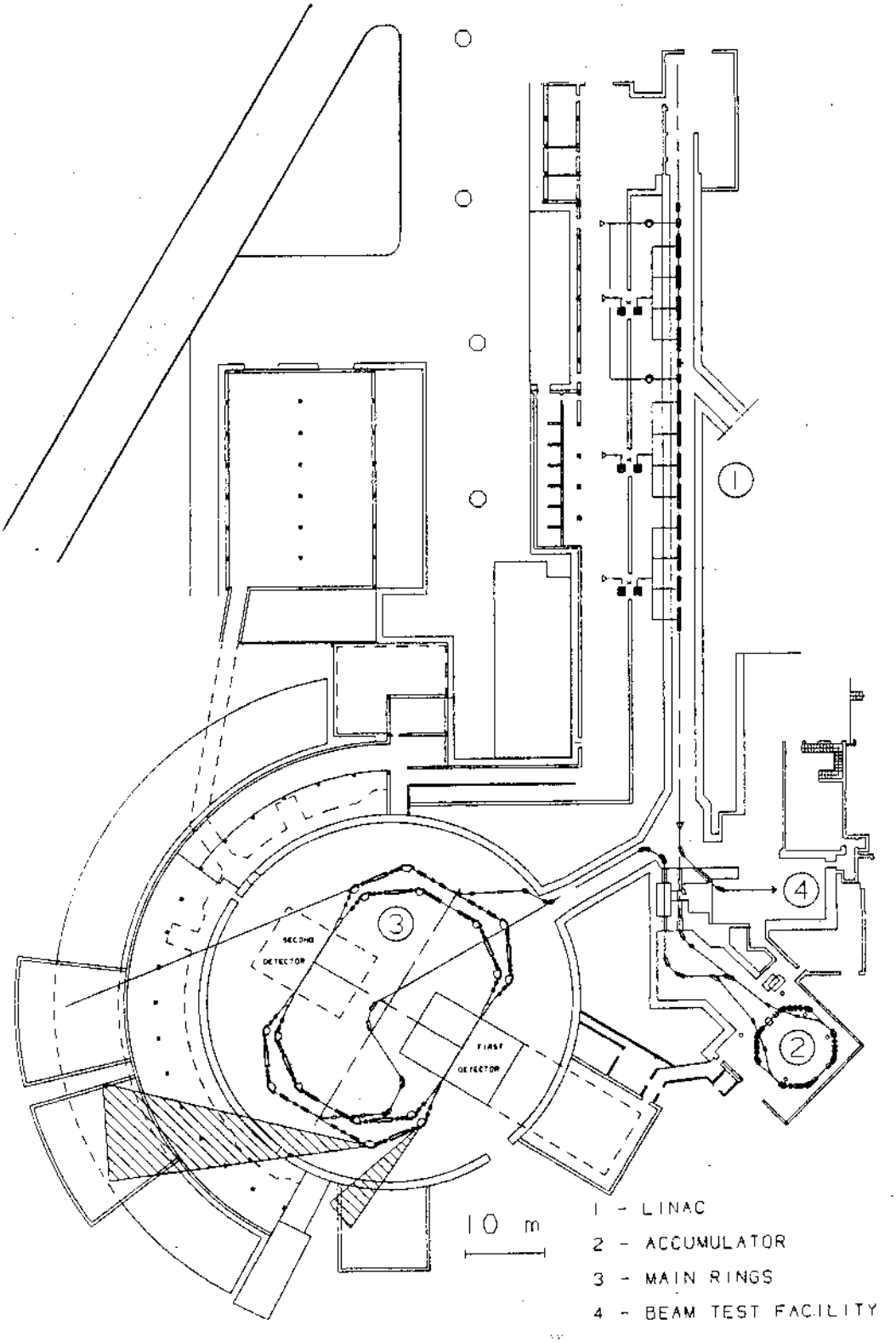

Figure 1. DAΦNE General Layout.

First of all, let us point out that the highest luminosity reached up to now in the existing machines, at the Φ energy,with flat beam and two interactions per turn, is

$$L = 4.3\ 10^{30}\ cm^{-2}\ sec^{-1}$$

at VEPP-2M in Novosibirsk, where there is an on-going effort to push up by a factor 2 this limit. Therefore, also our initial luminosity goal is very challenging and one has to be very careful in the fundamental choices.

The nature of a 'factory' in itself dictates an optimization of the luminosity at the operating energy. This process leads, anyway, to adopt a design in which all the parameters are chosen in such a way that the collider works near to the space charge limit in both planes. Under this assumption, the luminosity per interaction point (given by the number of bunches h multiplied the single bunch luminosity L_o), can be written as :

$$L = h\ L_o = \pi \left(\frac{\gamma}{r_e}\right)^2 h\ f_o\ \frac{\xi^2 \varepsilon (1+\kappa)}{\beta_y}$$

where γ is the electron energy in units of its rest mass, r_e the classical electron radius, h the number of bunches, f_o the revolution frequency, β_y the value of the vertical β-function at the IP, ξ the linear tune-shift parameter, ε the emittance and κ the coupling coefficient.

By inspecting the formula above, one can see that, for a given luminosity, there are two basic alternatives :

- small ring footprint and few bunches;
- larger ring footprint and many bunches.

The first alternative, that is pursued with different approaches in many Φ-factory designs (see these proceedings), is surely attractive from the accelerator physics and from the cost point of view, but it is also the most uncertain, since it requires single bunch luminosity L_o, which has never been achieved in the existing machines.

We have decided to adopt the second solution, with two separate storage rings in which electrons and positrons circulate in opposite directions and collide at a horizontal half angle θ_x = 10 mrad (in one or two interaction points), since it allows to reach the same luminosity without pushing L_o to very high values. The horizontal crossing, due to the values of the beam sizes at the interaction point, and to the reasonable value of the geometrical factor:

$$a = \theta_x\ \frac{\sigma_z}{\sigma_x} = 0.14$$

where σ_z = bunch length
σ_x = bunch width

should not excite synchrobetatron resonances [1] and it will allow to reach high collision frequency by filling, eventually, all the buckets.

An additional advantage of this choice is the possibility to build enough flexibility in the design, in order to allow the key machine parameters to be easily changed, to fine tune the luminosity as well as to test and to implement any new feature (round beam, zero momentum compaction, etc.) presently considered as a potential way to increase the luminosity. Moreover, the choice of a low L_o value helps in keeping the beam luminosity lifetime to a reasonable value (~ 20 hrs for DAΦNE).

The DAΦNE design parameters, relevant to the luminosity, are listed in Table I, while a

Table I - DAΦNE design parameters @ $\gamma = 1000$

$L_o(cm^{-2}\ sec^{-1})$	$4.5\ 10^{30}$
ξ	.04
ε^{max} (m-rad)	10^{-6}
κ	.01
β_y @IP (m)	.045
β_x @ IP (m)	4.5
N^{max} (particles/bunch)	$8.9\ 10^{10}$
h^{max} (N^{er} of bunches)	120
f_o(MHz)	3.17
σ_z (m)	.03

full discussion on their choice can be found in the original proposal [2]. These values indicate also other distinctive features of the design, like

- flat beam
- large emittance
- very high current.

Let us make one more comment upon the DAΦNE design parameters. The values of the parameters appearing in the luminosity formula are very similar to the VEPP-2M ones, with the exception of f_o, ε and the number of crossings (DAΦNE can operate with one crossing per turn). By properly scaling the VEPP-2M luminosity and by taking into account the improvement factor of 2, we get, with a certain dose of optimism

$$L_o = 7.2\ 10^{30} cm^{-2}\ sec^{-1}\ !$$

The DAΦNE expected luminosity, as function of the number of bunches for these two values of L_o, as well as the maximum current that is necessary to accumulate, are shown in Table II. It is evident that our choice, quite conservative from the single bunch luminosity point of view, is very demanding under other aspects, particularly for the very high current which is

needed in order to fill all the 120 buckets and the problems connected to. However these are technological single beam problems that can be solved.

Table II - DAΦNE luminosity and current vs. the number of bunches

h	$<i>^{max}$(Amp)	L ($cm^{-2}sec^{-1}$)	L ($cm^{-2}sec^{-1}$)
1	0.045	$4.50\ 10^{30}$	$7.20\ 10^{30}$
30	1.354	$1.35\ 10^{32}$	$2.16\ 10^{32}$
60	2.700	$2.70\ 10^{32}$	$4.32\ 10^{32}$
120	5.417	$5.39\ 10^{32}$	$8.64\ 10^{32}$

The design is based, as much as possible, on conventional technology. All the critical components (injector, vacuum system etc.) will be dimensioned to cope with the target luminosity of 10^{33} cm^{-2} sec^{-1}.

The parameters shown in Table I are the reference ones, and our commissioning strategy will be to fully use the flexibility built in the storage rings design to fine tune all of them in order to maximize L_o and to try to go over the design value. At the same time by optimizing L_o, we will gradually increase the number of bunches. This will require a certain amount of R&D in order to properly cure the multibunch instability, which is the most harmful problem in the design of high current storage rings and the most serious limitation for the luminosity.

MAIN RINGS

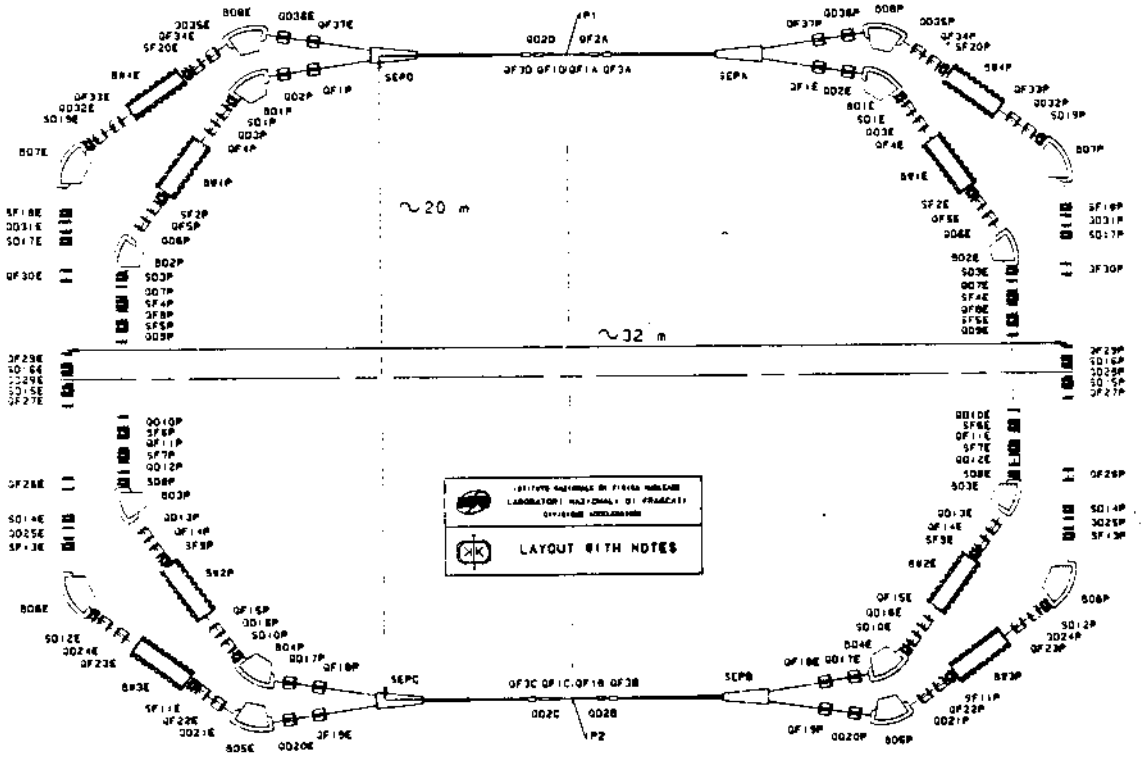

Figure 2. DAΦNE magnetic layout.

The DAΦNE magnetic layout is shown in Fig. 2. The lattice is a four-period modified Chasman-Green type. In order to increase the radiated energy per turn, a 2 m long, 1.8 T normal-conducting wiggler is incorporated into each achromat. The emittance value can be adjusted by tuning the dispersion function in the wiggler region.

Two different solutions have been designed: a higher emittance one with $\varepsilon = 10^{-6}$, and a lower emittance one with $\varepsilon = 5 \times 10^{-7}$. Moreover, a lattice with a high momentum compaction, which is useful to increase the threshold for the longitudinal microwave instability, is under study.

In the following, the high emittance lattice [3] is described in detail. The optical functions of half ring are shown in Fig. 3, while the single ring parameter list is given in Table III.

Table III - DAΦNE single ring parameters list

Energy (MeV)		510
Circumference (m)		94.56
Dipole bending radius (m)		1.400
Wiggler bending radius(m)		0.94
Wiggler length (m)		2.0
Wiggler period (m)		.66
Horizontal β-tune		4.12
Vertical β-tune		6.10
Natural chromaticities:	Horizontal	-4.8
	Vertical	-17.8
Momentum compaction		.0068
I_2 (m^{-1})		9.69
I_3 (m^{-2})		8.05
Energy loss/turn (KeV):	Bend.magnets	4.27
	Wigglers	4.96
	Total	9.30
Damping times (msec): τ_S		17.2
	τ_X	35.5
	τ_Y	34.6
Natural emittance (m-rad)		10^{-6}
Relative rms energy spread		$3.94\ 10^{-4}$
β_Y @ IP (m)		.045
β_X @ IP (m)		4.5
σ_Y @ IP (mm)		.021
σ_X @ IP (mm)		2.11
κ		.01
Bunch length σ_Z (cm)		3.0
Crossing half angle (mrad)		10.0
f_{RF} (MHz)		380.44
Harmonic number		120
Number of bunches		1 ÷ 120
Maximum number of particle/bunch		9.10^{10}
Maximum bunch peak current (A)		57
Maximum average current/bunch (mA)		46
Maximum total average current (A)		5.5
Maximum synchrotron power/beam (KW)		75
V_{RF} (KV)	@ Z/n = 2 Ω	241
	@ Z/n = 1 Ω	122
Parasitic losses @ σ_Z = 3 cm (KeV/Ω)		7

Let us point out that the values of I2, I3 and the other related quantities are somewhat less than the values given in [2]. This is due to the fact that we are using more realistic magnetic field profiles and we are taking into account the fringing fields.We are considering the possibility to insert a short S.C. wiggler in the long straight in case it turns out that more damping it is necessary, .

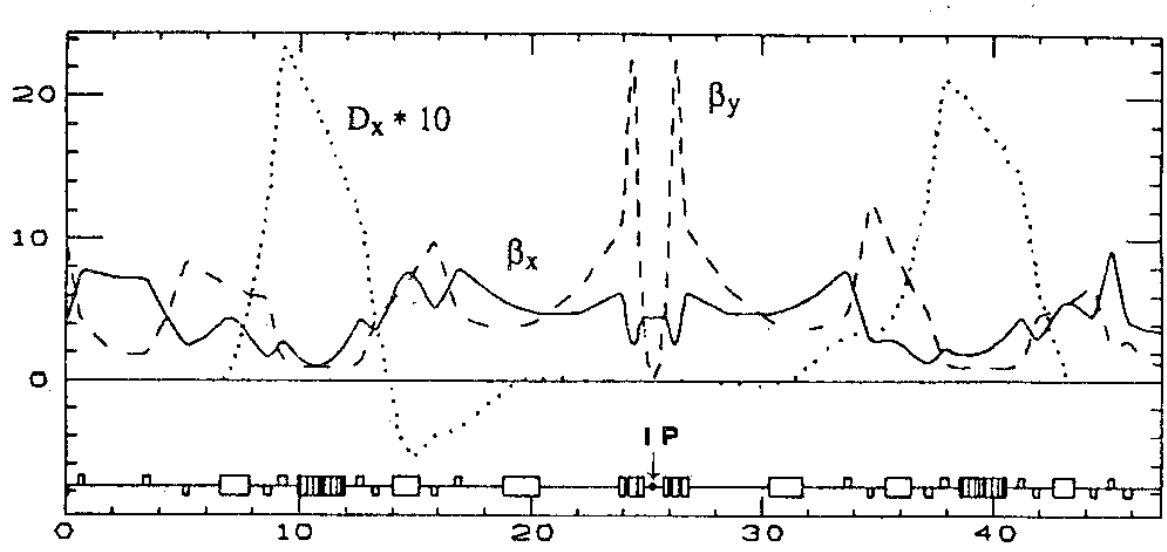

Figure 3. Optical functions of half ring.

A. Low-β insertion

The low-β insertion is one of the most crucial parts of the Φ-Factory design, because of the constraint imposed by the experimental apparatus, that is the requirement of a large unencumbered solid angle around the interaction point (IP). A tentative agreement has been reached with the users on a low-β insertion confined within a cone of half-aperture angle 8.5°, over a length of ± 5 m from the IP. The distance of the first quadrupole from the IP is 43.3 cm and the quadrupole maximum outer diameter $Ø_Q$ is 12.9 cm. Another constraint is the horizontal separation required at a short distance from the IP, to allow for a short bunch-to-bunch longitudinal distance L_b.

The optical parameters at the IP relevant to the luminosity are the following:

$$k_\beta = \frac{\beta_y^*}{\beta_x^*} = .01 \qquad \beta_y^* = .045 \text{ m} \qquad \beta_x^* = 4.5 \text{ m}$$

The low-β insertion consists of a quadrupole triplet followed by a long drift and a special design split field magnet. The first quadrupole is rather weak and focussing in the horizontal plane. This provides better control over the β functions and it keeps the horizontal beam size small inside the quadrupole triplet and along the rest of the insertion.

Let us point out that the low-β insertions give the largest contribution to the ring chromaticity; in particular the vertical chromaticity is Q'_y = -10.32 for the two insertions compared with Q'_y = -17.76 for the whole ring.

The half separation Δx between the two beams along with the horizontal beam size in the low-β insertion are plotted in Fig. 4. In the same figure the first parasitic crossing points for a filling of 30, 60, 120 buckets are indicated.

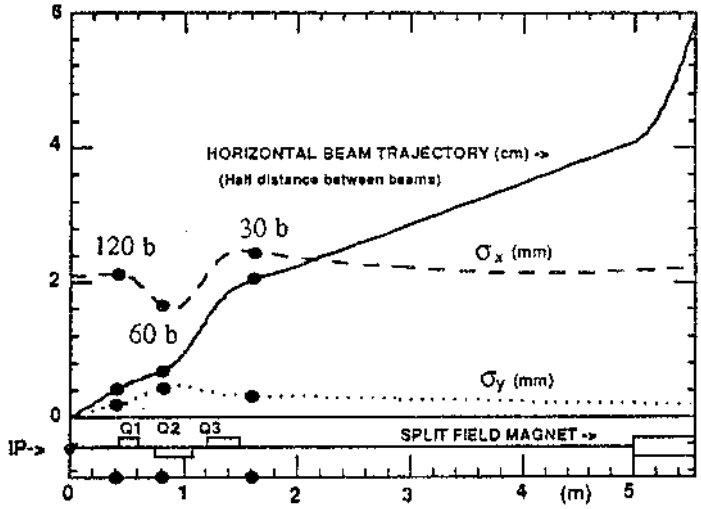

Figure 4. Beam half-separation and beam dimensions in the low-β region.
The heavy dots mark the parasitic crossing points.

The effect of the solenoidal field of the experimental apparatus will be corrected by means of six skew quadrupoles. Such a system, as suggested by M. Bassetti, will be used also as a local corrector to exactly overlap, in the vertical plane, the two intersecting beams.

B. Achromats

The low-β insertion is connected to the main arcs by a matching section, which consists of a long drift and two quadrupoles. The length of the drift is chosen in order to have a good separation between the first quadrupoles of the two rings. In this section, at π/2 horizontal betatron phase advance from the IP, there is room for a crab-cavity if necessary [1].

The dispersion and the horizontal β-function in the wiggler magnet are adjusted in order to tune the emittance without affecting the damping times, considering negligible the contribution of the bending magnets to the emittance.

C. Zero dispersion insertions

The change of the betatron tunes is done in the zero dispersion insertions. The short insertion has a 2.6 m long drift space with rather small β_X, suitable for the RF cavity. The long insertion provides space for injection septum and kickers, diagnostics and also free space for future developments.

D. Dynamic aperture

The study of the dynamic aperture has been performed with the computer code Patricia [4]. The strong sextupoles needed to correct the high vertical chromaticity are indeed the main limiting effects on the dynamic aperture.

To correct the tune-shift for particles with large oscillation amplitudes, a careful sextupole optimization in the dispersion-free regions has been performed.

The dynamic aperture is shown in Fig. 5, where the stable area for off-momentum particles, with a deviation $\Delta p/p = -.5\%$ (dashed line) and $\Delta p/p = +.5\%$ (dot-dashed line), are plotted for comparison on the unperturbed one (solid line).

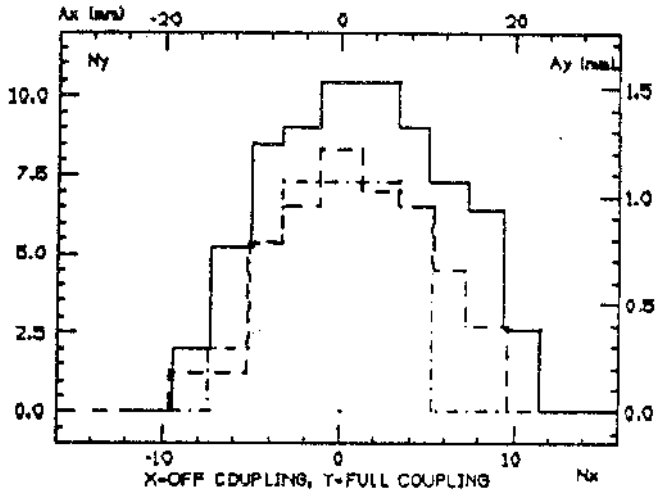

Figure 5. Dynamic apertures.

INJECTION SYSTEM

The maximum number of particles in each ring exceeds 10^{13}, thus setting challenging requirements on the design of the positron injection system. Since the operating time structure of the bunch configuration will be chosen upon the results of the machine commissioning, single bunch injection has been foreseen, so that the use of a small full energy storage ring, serving as an accumulator between a positron/electron Linac and the main ring, is the only possible solution to store the whole charge in the required injection time of ≈10 minutes. In order to mantain a high average luminosity, topping-up will be performed when the stored current drops below a given level, so that full injection will be necessary only at machine start-up.

Particles accelerated from the Linac will be injected at 50 Hz into the accumulator, extracted at 1 Hz and injected into the main rings, filling one bucket at a time. In order to reach the maximum design positron current, 360 pulses will be transferred from the accumulator to the main ring. Injection rate is foreseen to be much faster in the case of electrons and this is due to the larger current from the Linac.

A. LINAC

The S-band conventional Linac consists of a high current TW electron Linac with output energy ≥ 250 MeV, followed by an electron-positron converter, and low current e^-e^+ TW Linac with energy ≥ 510 MeV. A gridded gun, dimensioned for the maximum current required for positron production, will be used for both operating modes.

The bunching system will consist of a TM010 single cell cavity prebuncher and a 10÷20 MeV buncher with few graded β cells. The buncher length will be about 1÷1.5 m. The purpose of the system is to bunch the 'continuous' electron current emitted by the gun in a train of micropulses which corresponds to less than 15 degrees of the period of the Linac radiofrequency, and to accelerate the electrons to relativistic velocities before injecting them into the constant phase velocity (v=c) accelerating structure of the Linac.

According to the analysis presented in [5] we plan to adopt 2π/3 travelling wave (TW) constant gradient (CG) accelerating structures together with a SLED type pulse compression system. Such structures have been successfully tested in large size accelerators like SLAC, DESY and LEP.

The Linac will be installed into the 70 m existing tunnel of the ADONE Linac. Assuming a Linac filling factor 0.7, the total length of the accelerating sections should be around 50 m corresponding to a field gradient of about 20 MV/m. Our analysis shows that the optimum section length is 3 m.

The main components of the positron source are: the converter, the magnetic focusing and the high gradient capture accelerating section. The converter will be made of high Z materials such as Ta or Au, resistant to thermal and mechanical stresses. The average power of the electron beam passing @ 250 MeV through the converter will be about 1.2 kW, the power dissipated in the converter being about 16% (ie. ~ 200 W) of the total beam power.

The electrons will be focused by a quadrupole triplet to form a spot with a diameter ~ 1 mm, the positrons will be confined by a very intense tapered magnetic field of the order of 5÷6 Tesla generated by a flux concentrator [6]. Further optimization of the capture efficiency can be obtained by adding after the flux concentrator a short very high gradient accelerating capture section with the proper phase [7].

B. Accumulator

The use of an accumulator between the Linac and the main rings has the following major advantages:

- it avoids injection saturation due to the large number of injection pulses (≈1.6 10^4) by subdividing them into 45 pulses into the accumulator times 360 pulses into the main rings;
- it provides a larger longitudinal acceptance, since the RF frequency of the accumulator can be much lower than the main ring one;
- it decouples the design of the main rings from injection requirements, since the emittance and energy spread of the damped beam from the accumulator are much smaller than those of the beam coming directly from a Linac.

The length of the accumulator has been chosen as 1/3 of the main ring circumference, to easily synchronize injection of any desired bucket of DAΦNE. For the same reason, the RF frequency of the accumulator cavity is exactly 5 times lower than the main ring one.

Fig. 6 shows the layout of the positron/electron accumulator with the schematic of the transport channels from the Linac and to the main rings. Positrons will be injected into the accumulator from the left channel and extracted from the right one, while electrons will follow the opposite path. A symmetric set of four kickers will provide the necessary orbit distortion for injection and extraction of both electrons and positrons.

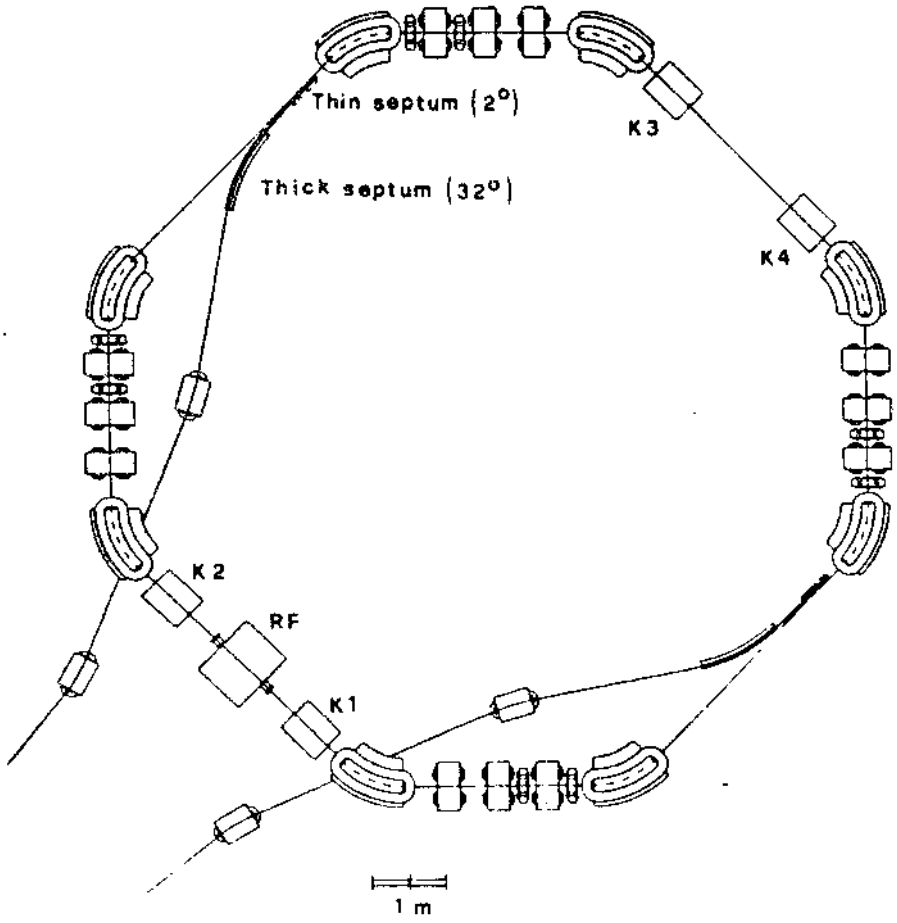

Figure 6. The Accumulator Layout.

The accumulator lattice, which derives from the storage ring ACO in Orsay [8], has a fourfold symmetric periodicity, and it has been chosen to optimize injection performance. The optical functions of one fourth of the ring are shown in Fig. 7.

Four low-dispersion 3.6 m long straight sections provide enough space for the kickers, the injection septa and the RF cavity. Each bending section includes two 45° magnets with field index n=0.5 to ensure the best damping partition, a quadrupole triplet to tune the horizontal phase difference between the kickers and the septa and a couple of sextupoles to correct the chromaticity in both the horizontal and the vertical plane.

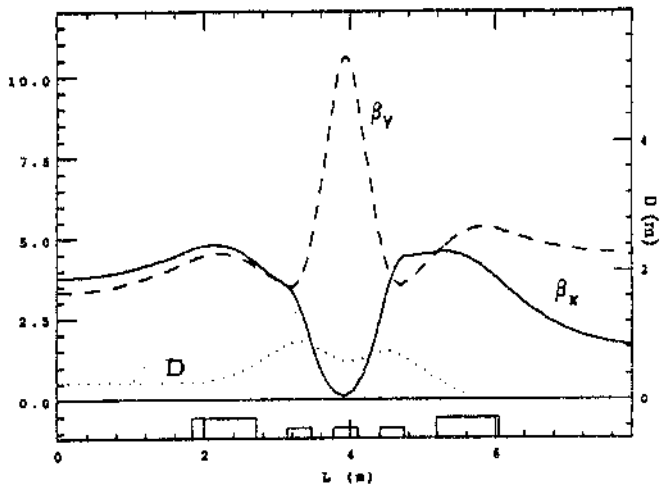

Figure 7. Optical Functions of one fourth of the Accumulator.

The gradient bending magnets will be H-shaped with a bending radius of 1.1 m, corresponding to a centre magnetic field of 1.55 T, with a minimum gap of 5 cm. The quadrupoles are designed to a magnetic length of 34 cm, with a maximum gradient of 8.3 T/m and a bore radius of 5 cm. The sextupoles have a magnetic length of 10 cm, with a maximum gradient of 110 T/m^2. Four kickers are used simultaneously for injection of electrons and positrons from the Linac. Only two of them provide the necessary kick to extract the beam from the accumulator. The required kicker pulse length is ≈100 nsec and the maximum strength is 85 G·m for injection and 139 G·m for extraction. Table IV gives a parameter list for the accumulator.

Table IV - Parameters of the Accumulator

Energy (GeV)	0.51
Circumference (m)	31.52
Straight section length (m)	3.67
Horizontal betatron wavenumber	2.89
Vertical betatron wavenumber	1.13
Horizontal betatron damping time (msec)	19.71
Vertical betatron damping time (msec)	19.71
Synchrotron damping time (msec)	9.86
Momentum compaction	0.047
Emittance (mm·mrad)	0.30
r.m.s. energy spread (%)	0.042
Horizontal chromaticity (sextupoles off)	-4.55
Vertical chromaticity (sextupoles off)	-4.10
RF frequency (MHz)	76.09
RF voltage (MV)	0.2
Harmonic number	8
RF energy acceptance (%)	±1.5%
r.m.s. bunch length (cm, radiation only)	1.81

STATUS OF THE PROJECT

The engineering design of vacuum and magnetic components, diagnostics, power supplies of the accumulator ring and of the main rings is in progress. The first prototypes will be built in the next few months.

Our main concern, at this time, is how to handle the multibunch instability. The parasitic high order modes of the RF cavities are responsible of such instability. The instability growth rate must be kept below the damping rate induced by the radiation. This can be obtained trough feedback system and proper RF cavity design.

We are designing a broadband (~50 MHz) feedback system with a damping time in the range of hundreds of μsec. Such system should allow, at machine start-up, to store 30 bunches if we have been able to design a good RF cavity. For this reason we have started a heavy R&D program on the resonators which is discussed in more details in the next paragraph.

We are also defining the engineering details of the interaction region. The aperture of the first three quadrupoles has to allow for good beam lifetime, moreover the beam separation and, at the same time, the outer dimensions are restricted by the experimental apparatus. Figure 8 shows a section of a permanent magnet hybrid-type quadrupole that we are building in collaboration with Ansaldo-Ricerca: this kind of magnet seems a good candidate for the IR quadrupoles and we will perform magnetic measurements next summer.

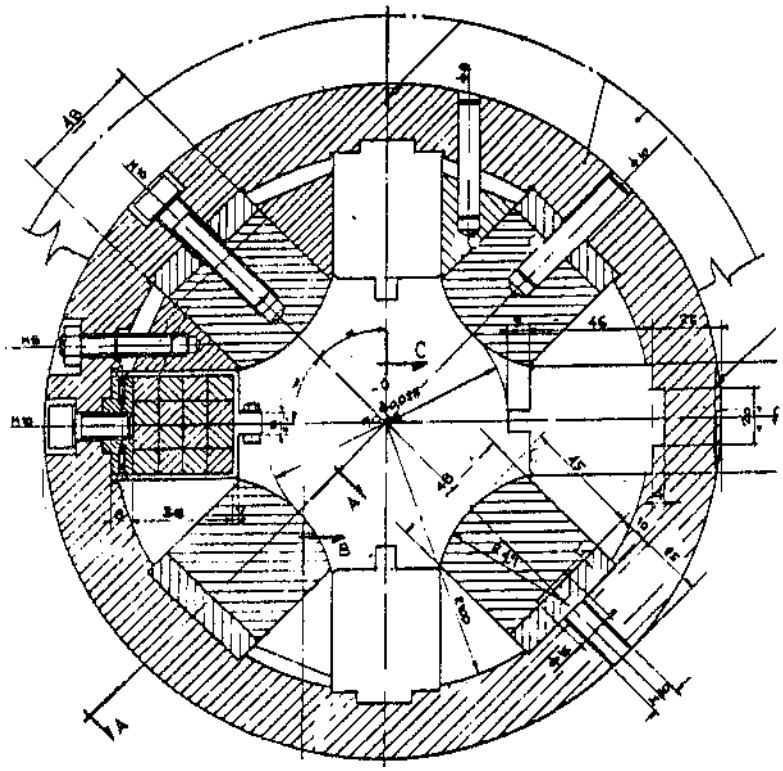

Figure 8. Permanent magnet hybrid-type quadrupole (section).

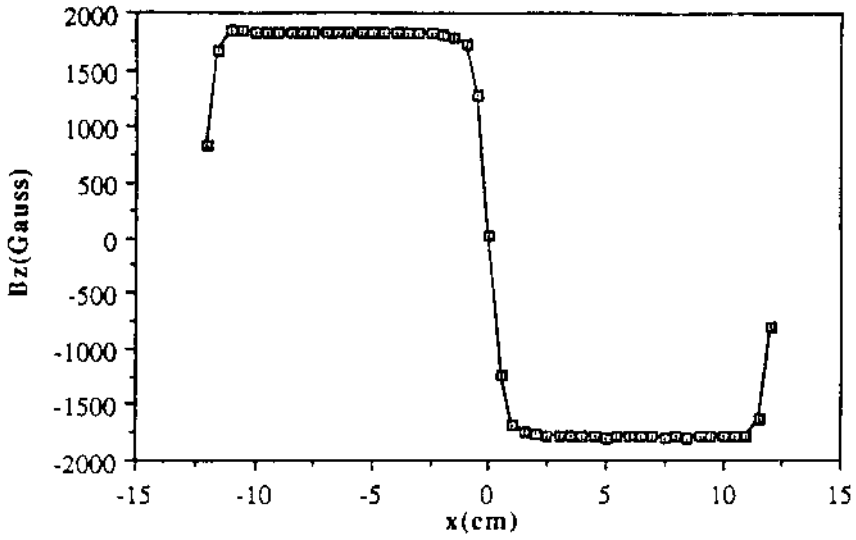

Figure 9. Computed magnetic field at the centre of the split field magnet.

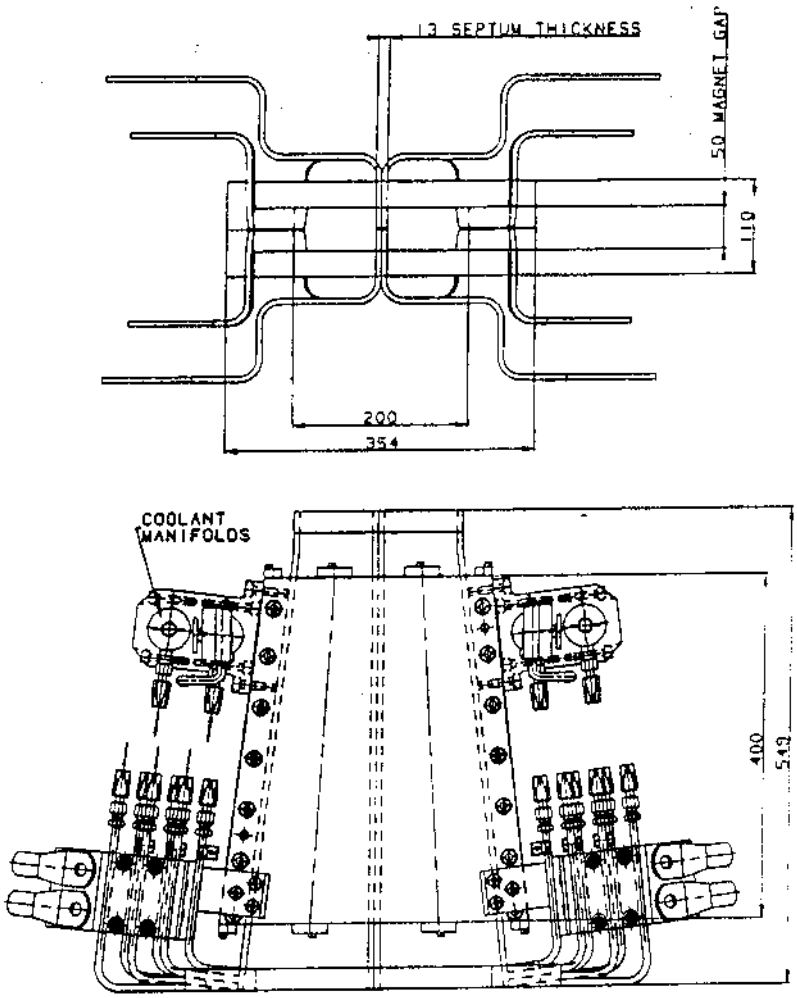

Figure 10. Engineering design of the split field magnet prototype.

Figure 9 shows the magnetic field at the centre of the split field magnet as predicted by the 3D Magnus code calculations. The field quality of this magnet is very sensitive to the coil positioning and we are building a prototype whose engineering design is shown in Fig. 10.

RF CAVITY R&D

Due to the high number of bunches, the higher order modes (HOM) in the RF cavities can excite multibunch instabilities. An intense R&D program, for the design of an RF cavity with the lowest interaction with the beam spectrum, is in progress.

Two different approaches have been followed:

a) coupling off and damping the higher order modes (HOM's) with absorbers;
b) shifting the HOM's frequencies while keeping that of the fundamental mode constant.

One method which has been recently proposed for coupling off the HOM's [9-10] consists in connecting one or more waveguides to the lateral surface of the resonator. The waveguide cut-off wavelength has to be higher than the fundamental mode wavelength in order to let it trapped in the cavity, whereas the HOM's are free to propagate out. A 380 MHz brass cavity prototype has been tested. Two waveguides are connected to the resonator and a dissipative load is placed at the other end of each guide.

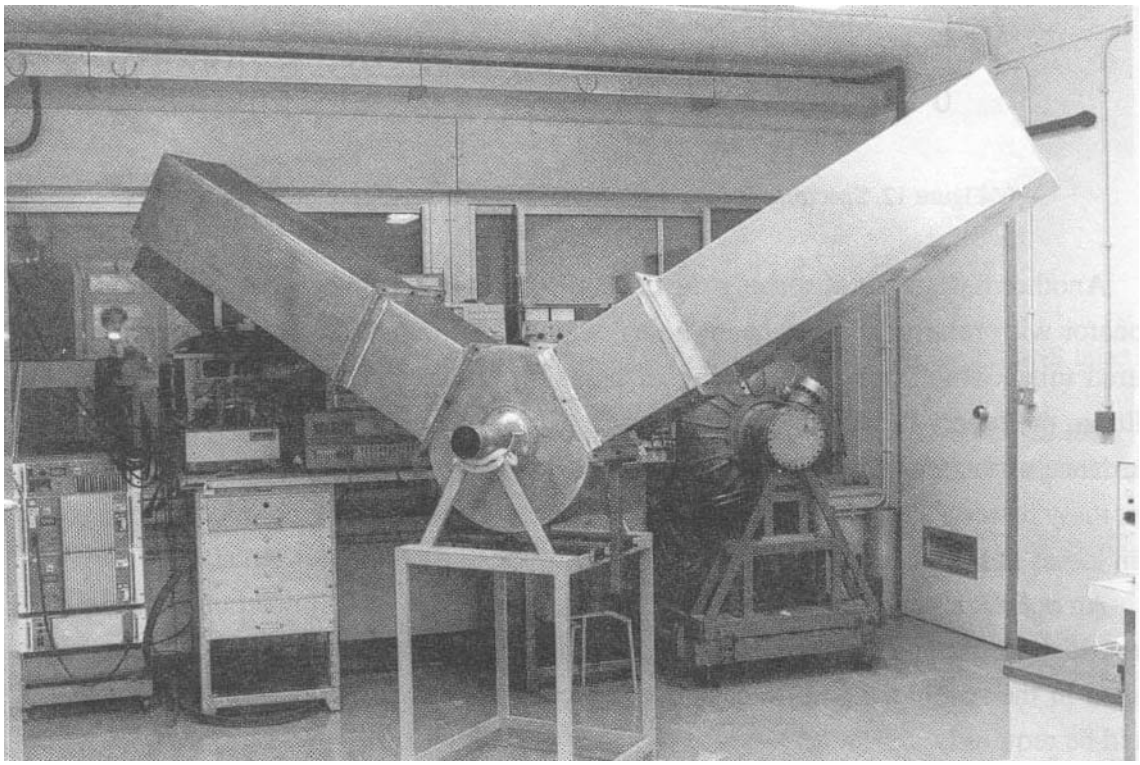

Figure 11. RF cavity prototype.

Figure 11 shows a first prototype of the RF cavity for low power test while in Fig. 12 the measured spectrum of the unperturbed prototype, and that of the waveguide-loaded cavity are compared. The measured reduction is 12 % for the fundamental mode frequency, and 25% for Q_o. The few remaining modes have a residual Q of some hundreds.

Some technological problems remain open: due to the pill-box shape which ensures the best coupling with the guides, the cavity is, in principle, prone to multipacting. Anyway, with an appropriate surface coating, multipacting can be inhibited. Furthermore, each damping load will dissipate a fraction (some kW's) of the parasitic beam losses and therefore an adequate cooling must be provided. In alternative to the present design, the use of ridged waveguides will be investigated in order to reduce the overall size of the cavity.

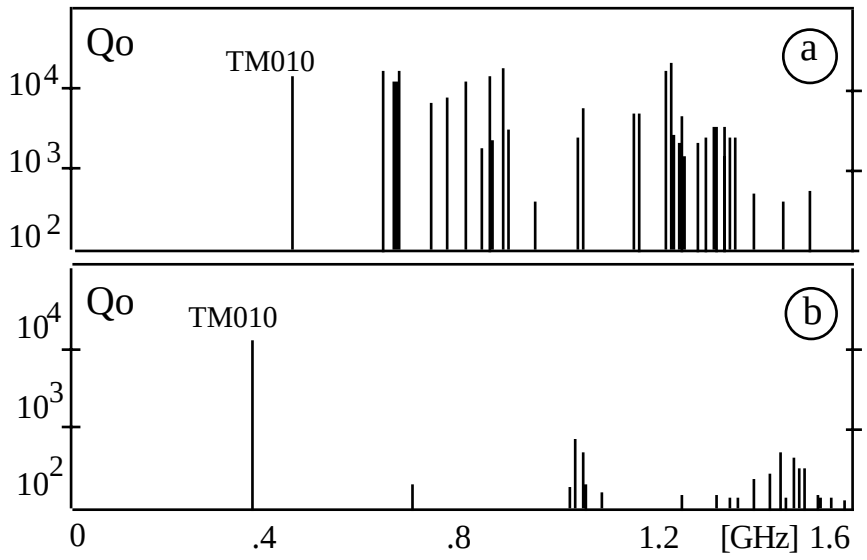

Figure 12. Spectrum of the uncoupled (a) and coupled (b) prototype cavity.

Another design for absorbing the cavity HOM's is being investigated. It consists of a resonator with relatively large beam holes, which is connected to the beam pipe with long tapered tubes which prevent trapping of parasitic modes in the resonator region [11]. In addition, the tapers reduce the cavity loss factor with beneficial effects on the broad-band impedance of the machine. However, the HOM's have to be damped by means of ferrites or other lossy materials located inside the tapered tubes and the heating produced by the parasitic beam losses has to be removed.

An optimization of the tapered profiles has been carried out. Simulations with TBCI [12] give a loss factor of about 0.12 V/pC/cell. Two parasitic dipole modes, however, remain trapped in the resonator and, in case they overlap the beam spectrum lines, then detuning would be required.

In Fig. 13 the long-tapered cavity profile is outlined along with the electric field lines of the fundamental mode.

An alternative way to fight collective coupled-bunch instabilities consists in shifting the HOM frequencies, without affecting the fundamental one, by means of perturbing metallic objects properly located [13]. Indeed, in small ring accelerators like DAΦNE, the spacing of beam spectrum lines is of the order of several MHz, so that the shift of a few offending HOM's can be a very powerful technique to decouple the beam oscillation modes from the cavity modes. The feasibility of this method is under study: one has to focus on the most dangerous cavity HOM's and to carefully consider the influence of the cavity tuning system at the injection.

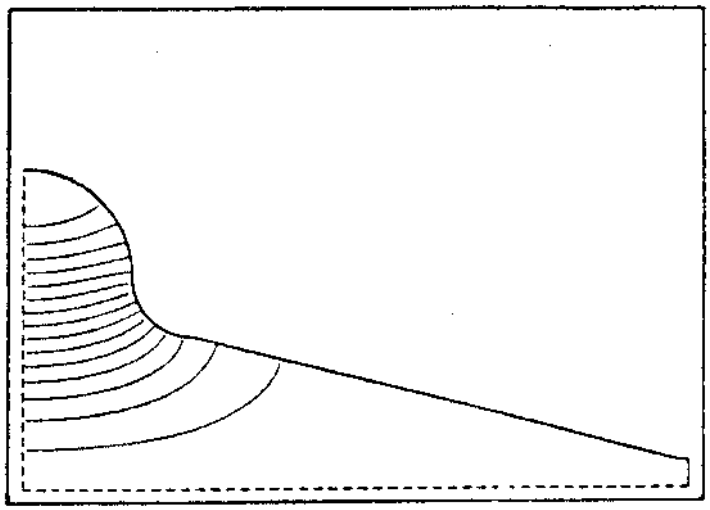

Figure 13. One quadrant of the long-tapered cavity.

REFERENCES

[1] S. Bartalucci et al., DAΦNE Technical Note G-1, (1990).

[2] "Proposal for a Φ-Factory", LNF-90/031(R), 1990.

[3] M. Bassetti et al., DAΦNE Technical Note L-1, (1990).

[4] H. Wiedemann, SSRL ACD-Note 29, (1985).

[5] S.Kulinski, R.Boni, B.Spataro, M.Vescovi, G.Vignola, "The Linear Accelerator for DAΦNE Injection System", DAΦNE Tech. Note, LC-1, Febr. 1991.

[6] D. Sherden, "Tapered Solenoid for SPC Positron Source", SLC Design Book, MEMO CN-22.1980.

[7] B. Aune and R.H. Miller, "New Method for Positron Production at SLAC", SLAC PUB. 2393 Sept. 1979.

[8] P.Marin et al., "Status Report on the Orsay Electron Positron Storage Ring", VI Int. Conf. on H.E.A. Cambridge 1967.

[9] G. Conciauro, P. Arcioni, Proceedings of EPAC 90, Nice, France,1990, p. 149, (1990).

[10] A. Massarotti, M.Svandrlik, Sincrotrone Trieste, Note ST/M-90/5, (1990).

[11] T.Weiland, DESY 83-073, (1983).

[12] T.Weiland, DESY 82-015, (1982).

[13] S. Bartalucci et al., "A Perturbation Method for HOM Tuning in a RF Cavity", submitted for publication to N.I.&Meth.